JOURNAL OF Materials CHEMISTRY

The ageing of alumina hydrolysates synthesized from *sec*-butoxyaluminium(III)

W. N. Martens,[a] R. L. Frost,*[a] J. Bartlett[b] and J. T. Kloprogge[a]

[a]*Centre for Instrumental and Developmental Chemistry, Queensland University of Technology, 2 George Street, GPO Box 2434, Brisbane, Queensland, 4001, Australia. E-mail: r.frost@qut.edu.au*
[b]*Materials Division, Australian Nuclear Science and Technology Organisation, Private Mail Bag 1, Menai, NSW, 2234, Australia*

Received 19th December 2000, Accepted 13th March 2001
First published as an Advance Article on the web 5th April 2001

A combination of X-ray diffraction, thermal analysis and Raman spectroscopy was employed to characterise the ageing of alumina hydrolysates synthesised from the hydrolysis of anhydrous tri-*sec*-butoxyaluminium(III). X-Ray diffraction showed that the alumino-oxy(hydroxy) hydrolysates were pseudoboehmite. For boehmite the lamellar spacings are in the *b* direction and multiple *d*(020) peaks are observed for the un-aged hydrolysate. After 4 h of ageing, a single *d*(020) peak is observed at 6.53 Å. Thermal analysis showed five endotherms at 70, 140, 238, 351 and 445 °C. These endotherms are attributed to the dehydration and dehydroxylation of the boehmite-like hydrolysate. Raman spectroscopy shows the presence of bands for the washed hydrolysates at 333, 355, 414, 455, 475, 495, 530 and 675 cm^{-1}. These bands are attributed to pseudoboehmite. Ageing of the hydrolysates results in an increase in the crystallite size of the pseudoboehmite.

1 Introduction

Alumina obtained through sol–gel processing is one of the most important ceramics used commercially today. Its uses include abrasives, refractories, chemical-resistant coatings, bioceramic implants and integrated circuit substrates. Thus it is important that the structure of alumina formed *via* the sol–gel process must be adequately studied. Alumina hydrolysates, sols and gels are readily prepared by the hydrolysis of aluminium alkoxides such as tri-*sec*-butoxyaluminium(III) (ASB).[1,2] Several phases of aluminium (oxy)hydroxides exist according to the formula $Al(OH)_3$; these are gibbsite, nordstrandite and bayerite.[3] If the phase corresponds to the formula AlO(OH), then the phases are boehmite or diaspore.[3] Pseudoboehmite is a hydrated form of boehmite with slightly larger *d*-spacing. The chemical and structural make-up of the oxo-hydroxides formed from the hydrolysates depend on the conditions of the hydrolysis and the ageing of the hydrolysates.[4,5] Ageing simply means that changes in phase are brought about as either the hydrolysate or gel is left to stand in the presence of water. Such ageing can affect the rates of peptisation of the alumina sols. Ageing of the oxo-hydroxides as gels causes structural changes in the sequence amorphous–pseudoboehmite–bayerite–gibbsite.[1,2] To date, little published research on the ageing of alumina hydrolysates and gels has been forthcoming.

It is often necessary to synthesise alumina ceramics with tailored properties for particular applications, for example, for the slow release of drugs using a porous alumina ceramic. In these instances the control of the reaction kinetics of hydrolysis and condensation is important. For the manufacture of these types of material it is useful to modify the alkoxide precursors. Modification of precursors can be performed by co-ordination of the starting material with ligands. Metal alkoxides react with ligands because of their co-ordination unsaturation. For this to occur the metals expand their co-ordination *via* a nucleophilic addition. Such ligands as alcohols and acids may be used to react with the ASB. Chemical modifiers are substances which are used in controlling or retarding the rate of hydrolysis and condensation so that the desired material is formed whether it a gel, colloidal solution or precipitate.[6,7] The methodology is essential in the process of obtaining a metal sol that is suitable to be used in, for example, coating applications. Acids, chlorides, alcohols, bases and chelating agents are all substances that effectively produce a new, less reactive precursor.[8] Recent research has explored the thermal analysis of gels formed from the hydrolysates produced from tri-*sec*-butoxyaluminium(III) and also acid-modified ASB.[9,10] This research produced hydrolysates and gels from ASB but the ASB was not necessarily free of water. In order to ensure that the ASB remained uncontaminated by water, the ASB was distilled under nitrogen. It has been found by us that the kinetics of peptisation of the alumina oxy(hydroxides) are directly related to the structural characteristics of the hydrolysate. These structural characteristics are a function of temperature, particle size, included impurities such as *sec*-butanol, and water content. These structural characteristics change with time. Such a phenomenon is known as ageing. Thus, the objective of this research is to determine, using suitable techniques, the changes in the structure with time. This paper therefore reports for the first time the structural evolution of alumina oxy(hydroxides) through the ageing of hydrolysates formed from ASB at 75 °C using a combination of X-ray diffraction, thermal analysis and Raman spectroscopy.

2 Experimental

2.1 Synthesis of alumina hydrolysates

A solution of 0.1 M tri-*sec*-butoxyaluminium(III) (ASB) was prepared in anhydrous, doubly distilled dibutyl ether under a nitrogen atmosphere. This solution was then mixed slowly at 0 °C to form the modified ASB solution. This starting material was then added, under constant, vigorous stirring to demineralised water at 75 °C in a molar ratio of 1 : 100 alkoxide solution to water. A sample of each hydrolysate was taken for analysis. The resulting precipitates were washed several times with water to remove organic reaction products, namely

alcohol, and then diluted in water to give slurries with a concentration of aluminium of 1 : 100 Al : water molar ratio. Samples were dried under a nitrogen stream for 12 h before X-ray diffraction and Raman spectroscopic analysis.

2.2 Characterization

2.2.1 X-Ray diffraction. Normal room-temperature and temperature-controlled XRD analyses were carried out on a Philips wide angle PW 3020/1820 vertical goniometer equipped with curved graphite-diffracted beam monochromators. The *d*-spacing and intensity measurements were improved by application of a self-developed, computer-aided divergence slit system enabling constant sampling area irradiation (20 mm long) at any angle of incidence. The goniometer radius was enlarged from 173 to 204 mm. The radiation applied was Cu-Kα from a long, fine focus Cu tube operating at 40 kV and 40 mA. The samples were measured in static air and in a flowing nitrogen atmosphere at 15 l h^{-1} in stepscan mode with steps of 0.025° 2θ and a counting time of 1 s. Measured data were corrected with the Lorentz polarisation factor (for oriented specimens) and for their irradiated volume.

2.2.2 Thermal analysis. Differential thermal and thermogravimetric analyses of the hydrolysates were obtained simultaneously using a Setaram DTA/TGA instrument, operating with a heating rate of 1.0 °C min^{-1} from ambient temperatures to 1350 °C in an inert atmosphere. For comparison, a commercially available boehmite known as 'dispal' was used.

2.2.3 FT-Raman spectroscopy. All Raman spectra were obtained using a Biorad FT-Raman II spectrophotometer using a Spectra Physics Nd-doped YAG diode laser system operating at 1064 nm. The spectrometer used a NIR silica beam splitter with a holographic notch filter (−200 to 50 cm^{-1}). A liquid nitrogen-cooled germanium detector was employed. All samples were contained in mirrored-back capillary tubes, scanned 2048 times with a resolution of 4 cm^{-1} and a mirror velocity of 5 kHz using 180° optics.

Spectral manipulations such as baseline adjustment, smoothing and normalisation were performed using the GRAMS32® software package (Galactic Industries Corporation, Salem, NH, USA). Band component analysis was undertaken using the Jandel 'Peakfit' software package, which enabled the type of fitting and function to be selected and allowed specific parameters to be fixed or varied. Band fitting was done using a Lorentz–Gauss product function with the minimum number of component bands used for the fitting process. The Gauss–Lorentz ratio was maintained at values greater than 0.7 and fitting was undertaken until reproducible results were obtained with squared correlations of $r^2 > 0.995$ for the 298 K spectra. Graphics are presented using Microsoft EXCEL.

3 Results and discussion

The structure of sol–gel-processed alumina has received much attention. It has been found that amorphous aluminium oxy(hydroxide) is formed on the hydrolysis of ASB in water at 25 °C. This amorphous AlOOH undergoes ageing and forms pseudoboehmite then bayerite *via* a dissolution–re-precipitation process. When alumina, precipitated from the action of water on ASB at 75 °C, formed pseudoboehmite, no ageing process was seen. One such study was conducted by Pierre and Uhlmann.[11,12] Here, the authors postulated that the structure of the resultant AlOOH, formed from cold water hydrolysis of ASB, was that of a boehmite structure folded along the 020 planes. This structure was then proposed to straighten during ageing of the amorphous aluminium oxy(hydroxide), which results in the formation of pseudoboehmite. Such a structure showed an X-ray diffraction pattern with the (020) peak for pseudoboehmite but not other peaks: this was attributed to the disintegration of long range order but preservation of short range order. It should be noted that the temperature of hydrolysis is 75 °C, the reason being that at and above this temperature a single phase is formed. If the hydrolysate is formed at 25 °C, an amorphous aluminium oxy(hydroxide) is formed, which upon ageing transforms to boehmite and gibbsite. Further ageing of the mixture in the absence of alkali ions may bring about transformation to bayerite.[13]

3.1 X-Ray diffraction of alumino oxy(hydroxide) hydrolysates and gels

The structure of boehmite consists of double layers of oxygen octahedra partially filled with Al cations.[14] The stacking arrangement of the three oxygen layers is such that the double octahedral layer is in cubic closed packing.[14] Within the double layer one can discriminate between two different types of oxygen:[14] each oxygen in the middle of the double layer is shared by four other octahedra, whereas the oxygens on the outside are shared by only two octahedra.[14] These outer oxygens are hydrogen-bonded to two other similarly coordinated oxygens in the neighboring double layers above and below.[14] The crystal group of boehmite was determined to be D_{2h}^{17}-*Amam* by Reichertz and Yost[15] and later Milligan and McAttee[16] using XRD.

The X-ray diffraction patterns of alumina hydrolysates prepared from the reaction of tri-*sec*-butoxyaluminium(III) in anhydrous dibutyl ether and aged for a range of times, together with the XRD pattern of a standard boehmite, are shown in Fig. 1. For boehmite the lamellar spacings are observed along the *b* direction and consequently the *d*(020) is the principal first peak. The principal *d*-spacings for boehmite are observed at 6.15 (020), 3.14 (021), 2.33 (130), 1.84 (150), 1.45 (132), 1.43 (200) and 1.30 (221) Å. The published values for boehmite are 6.12, 3.16 and 2.34 Å. The hydrolysates at the different times of ageing all show a pattern similar to that of boehmite. For the unaged hydrolysate and up to 1 h of ageing, multiple *d*(020) peaks are observed. At zero time, peaks are observed at 6.24, 7.53 and 9.9 Å. At an ageing time of 0.50 h, three peaks are observed, at 5.72, 6.31 and 6.90 Å. After 1 h ageing time, peaks are observed at 6.14, 6.47 and 7.05 Å. After 4 h of ageing a single *d*(020) peak is observed at 6.52 Å. Fig. 2 shows the variation of the *d*-spacing and the peak width of the (020) peak with ageing time. Both these variables decrease with ageing time but do not reach the values for that of boehmite.

As the hydrolysates are first formed, these materials are amorphous or non-diffracting and contain many stacking defects along the (020) direction. As ageing occurs, bigger crystals are formed and these defects are removed. Hence a decrease in the peak width is observed. The differences are

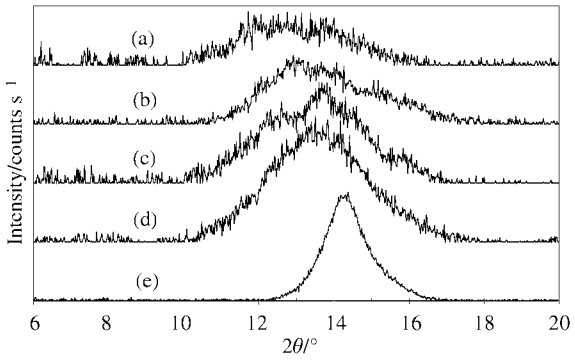

Fig. 1 X-Ray diffraction patterns of the *d*(020) spacing of aluminium oxy(hydroxide) hydrolysate (a) zero ageing time, (b) 0.5 h, (c) 1 h, (d) 4 h, (e) boehmite.

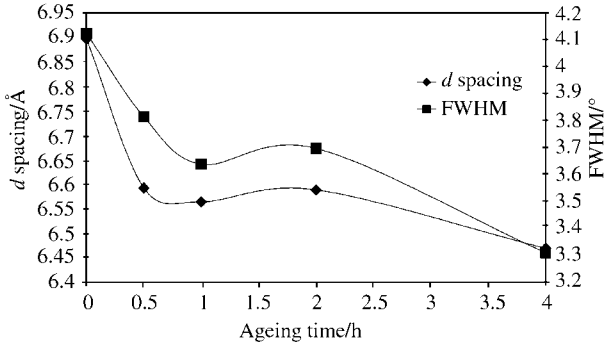

Fig. 2 Variation of *d*(020) peak position and peak width with ageing time.

attributed to the amount of water between the hydrolysate layers and the arrangement of these water molecules between the layers. The reason for the difference between the standard boehmite and the 4 h aged hydrolysate is attributed to the presence of water between the layers. The standard boehmite was spray dried and consequently most of the water has been removed. The kinetics of peptisation of these hydrolysates with nitric acid depend upon the ageing of the hydrolysates. The 4 h aged hydrolysate is the most easily peptised.

3.2 Thermal analysis

The differential thermal analysis patterns for a standard boehmite and an aged alumina oxy(hydroxy) hydrolysate (4 h sample) are shown in Fig. 3. Five peaks are observed in the thermal analysis patterns at around 70, 140, 238, 351 and 445 °C. The first two peaks (70 and 140 °C) are attributed to the endotherms of adsorbed water and water chemically bound to the boehmite surface. The third endotherm (238 °C) is of low intensity and may correspond to the endotherm of gibbsite. The last two endotherms (351 and 445 °C) are attributed to the two types of hydroxy group in the boehmite structure. The endotherm at around 351 °C is assigned to external hydroxys and the second boehmite peak at around 445 °C is ascribed to the hydroxy groups which bridge across adjacent boehmite layers.

As expected, there is much in common in the TGA and DTGA patterns of the aged hydrolysates and a standard boehmite. Three steps can be distinguished. Step 1 is attributed to the weight loss of water, and in this step between 21 (0 h) and 19% (4 h) by weight is lost. Whilst it is possible to distinguish between two steps in the DTA pattern for the endotherms attributed to water, in the TGA and DTGA patterns only a single step is observed. Steps 2 and 3 are attributed to the weight loss of the boehmite hydroxy groups. The weight loss in Step 2 is between 8 and 6.5% with a decrease observed with ageing time. The weight loss for Step 3 varies between 7 and 8.5% and increases with ageing time. The weight loss of water appears to decrease with ageing time. Such an observation is in accord with the results of the X-ray analysis where it was proposed that water was held in the interlayer spaces of the boehmite, thus resulting in several *d*(020) spacings. The decrease in the weight loss of Step 2 observed with ageing time is attributed to the loss of surface hydroxy groups. As the hydrolysates age, the boehmite layer stacking disorder decreases resulting in increased crystallinity of the boehmite. Considering the weight loss in Step 3, which increases with ageing time, we conclude from the results of the thermal analysis that the aged hydrolysates contain less water. The implication is that such hydrolysates will peptise more readily. Furthermore, the positions of the boehmite endotherms suggest that the ageing process creates bigger particles. The implication here is that the aged hydrolysates peptise more readily.

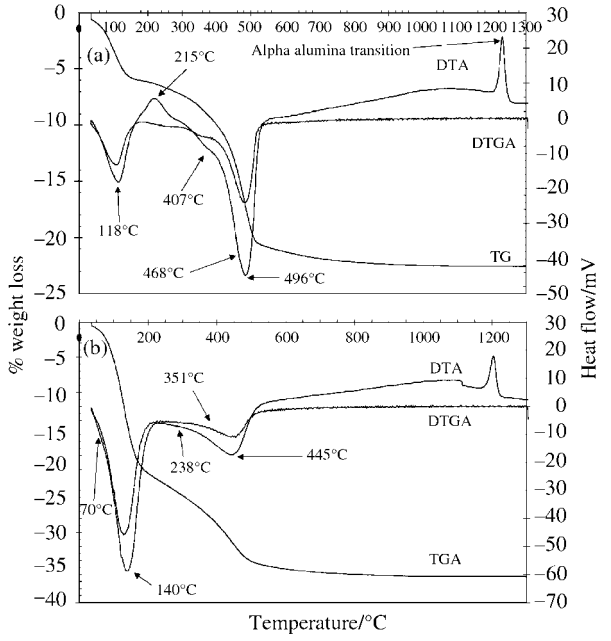

Fig. 3 (a) Thermal analysis of boehmite; (b) thermal analysis of hydrolysate formed at 75 °C and aged for 4 h.

3.3 Raman spectroscopy of boehmite and pseudoboehmite

Boehmite was found to have four AlOOH units per non-primitive unit cell in which all atoms lie in sites with C_{2v} symmetry (excluding hydrogens, which could not be determined).[17] Using this symmetry group Kiss *et al.*[17] determined that there are six IR- and nine Raman-active modes for the Al–O vibrations represented by the factor groups of $3A_g+3B_{1g}+3B_{2g}+2B_{1u}+2B_{2u}+3B_{3u}$ (ignoring acoustic modes). Using their model for the hydrogen bonding they calculated five IR- and six Raman-active modes represented by the factor groups $2A_g+2B_{1g}+2B_{2g}+2B_{3g}+A_u+B_{1u}+2B_{2u}+2B_{3u}$. This model requires the delocalisation of H^+ ions, which is supported by the peptisation of these materials. Kiss *et al.*[17] assigned the lattice vibrations as indicated in Table 1. Most authors agree that boehmite and pseudoboehmite have the same crystal structure, varying only in water content and degree of crystallinity. This extra water lies in the hydrogen-bonding layer of boehmite.[18–21] It swells the layer, which is detectable by the *d* spacing in the XRD pattern. An indication of crystallinity is the bandwidth of the Raman bands[21] – a large bandwidth usually indicates a large range of bond lengths and hence low crystallinity.

Table 1 Assignment of the vibrations of boehmite[17]

Band/cm^{-1}	Symmetry species	Description
3220	B_{1g}	$\nu_{as}OH$
3080	A_g	ν_sOH
1110	B_{1g}	$\delta_{as}OH$
1053	A_g	δ_sOH
733	B_{2g}	γOH
676	A_g	ν_2AlO_6 (E_g)
639	B_{1g}	ν_5AlO_6 (F_{2g})
497	A_g	ν_2AlO_6 (E_g)
454	B_{2g}	ν_5AlO_6 (F_{2g})
369	A_g	ν_1AlO_6 (A_{1g})
343	B_{2g}	ν_5AlO_6 (F_{2g})
272	B_{1g}	AlO_6 (F_{1g})
260	B_{2g}	AlO_6 (F_{1g})
232	B_{1g}	AlO_6 (F_{1g})

3.4 Raman spectroscopy of pseudoboehmite hydrolysates

The Raman spectra of the hydrolysates before and after washing are shown in Fig. 4 and 5, respectively. The results of peak fitting are reported in Table 2. Peak fitting is undertaken such that an r^2 value of >0.995 is obtained. Such peak fitting means that the difference between the experimentally obtained profile and the fitted profile is very small, and the fits are undertaken in such a way that consistency in peak position across all fitted profiles is obtained. The Raman spectra for the refluxed hydrolysates show seven peaks in the region 250–750 cm^{-1} and eight for the washed hydrolysates. In the region 1300–800 cm^{-1} the spectra of refluxed hydrolysates consist of ten peaks, which are attributed to *sec*-butanol formed from the hydrolysis of ASB. The Raman spectra of pseudoboehmite show seven main peaks, as reported by Assih *et al.*,[17] summarised in Table 1. Representative band fitted spectra are shown in Fig. 6 and 7, refluxed samples showing peaks at approximately 355, 390, 415, 440, 470, 501, 530 cm^{-1}

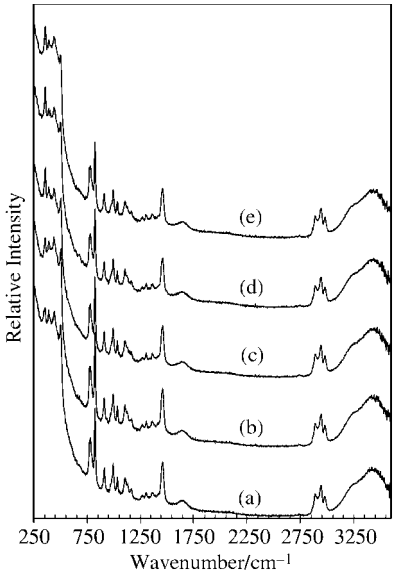

Fig. 4 Raman spectra of hydrolysates aged at 75 °C for (a) 0 h, (b) 0.5 h, (c) 1 h, (d) 2 h, (e) 4 h.

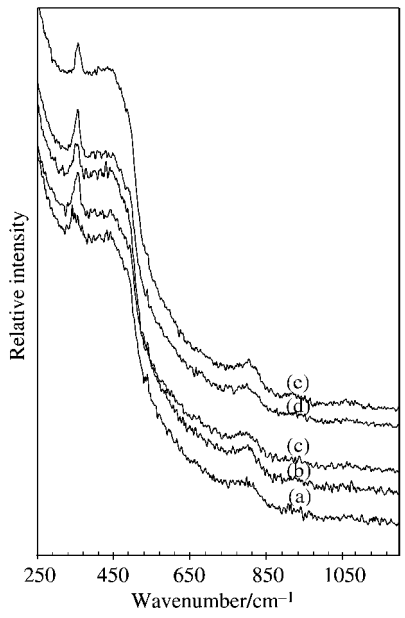

Fig. 5 Raman spectra of the washed hydrolysates aged at 75 °C for (a) 0 h, (b) 0.5 h, (c) 1 h, (d) 2 h, (e) 4 h.

and washed hydrolysates at 333, 355, 414, 455, 475, 495, 530, 675 cm^{-1}. The main difference in the spectra for washed and refluxed hydrolysates is evident by looking at the relative intensity of the strongest pseudoboehmite band at 355 cm^{-1}. According to Kiss *et al.*[17] this vibration of pseudoboehmite is due to the totally symmetric vibration of the AlO_6 octahedra in the boehmite structure. In washed hydrolysates this band is the most intense band. With refluxed hydrolysates, however, this band is less intense owing to the contribution of *sec*-butanol to the Raman spectrum. The Raman spectra of a 3 : 100 molar ratio of *sec*-butanol to water mixture show bands at 356 (broad weak), 390, 447 (broad), 502 and 562 (very broad weak) cm^{-1}. The bands at 447 and 552 cm^{-1} are assigned to the water libration modes with literature assignment for these bands at 450 and 550 cm^{-1}, respectively. The reason for not observing the pseudoboehmite bands at 333 and 675 cm^{-1} in the refluxed hydrolysates is due to the overlap of the broad band at 356 cm^{-1}, which is due to the *sec*-butanol with the weak band of pseudoboehmite at 333 cm^{-1}. In the refluxed hydrolysates an extra band attributable to *sec*-butanol is observed. It is seen for the band fitting of the Raman spectrum of a 3 : 100 molar ratio *sec*-butanol to water mixture that it is likely that *sec*-butanol contributes to bands at both 501 and 466 cm^{-1}.

The bandwidth (as FWHM) of the boehmite peak at 355 cm^{-1} in the spectrum decreases with ageing time (Fig. 8). This observation correlates with the results of dynamic light scattering. The ageing process seems to be finished by 1 h for hydrolysates hydrolysed and aged at 75 °C. It is also seen that the bandwidth of the 355 cm^{-1} band of the hydrolysates hydrolysed and aged at 85 °C shows that ageing is completed within 0.5 h. This would be expected if the reaction kinetics of the ageing process were first order, as a 10 °C increase in temperature would result in a doubling of the rate of reaction. The increase in crystallinity observed through the decrease in the bandwidth of the 355 cm^{-1} Raman band can be used to

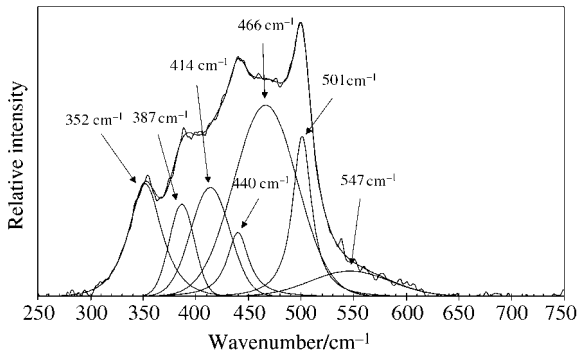

Fig. 6 Band component analysis of the Raman spectrum of an un-aged refluxed hydrolysate formed at 75 °C.

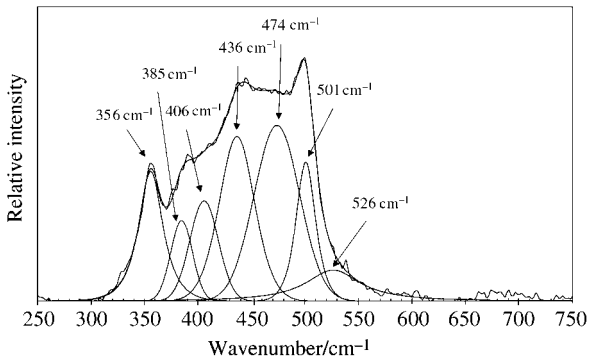

Fig. 7 Band component analysis of the Raman spectrum of a 4 h aged refluxed hydrolysate formed at 75 °C.

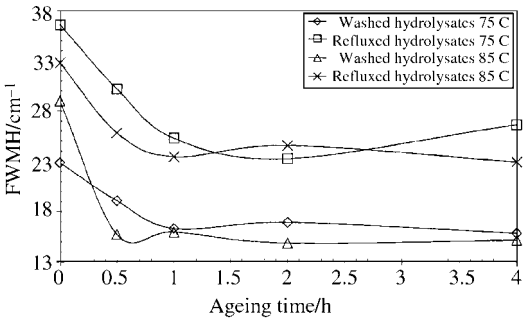

Fig. 8 Variation of the bandwidth of the 355 cm^{-1} peak as a function of ageing time.

explain the increased peptisability of the hydrolysates. The experiments conducted by Zakharchenya[18] revealed that peptisation caused an increase in the hydrogen bond strength in the pseudoboehmite seen by a reduction in the inter-planar distances in the pseudoboehmite hydrolysates. It was hypothesized that peptisation results in the removal of inter-planar water, which would give the decrease in the crystal spacing as observed by XRD along the 010 plane of pseudoboehmite. Zakharchenya postulated that surface charge formation caused a redistribution of electron density in boehmite, which results in an increase in the hydrogen bonding between crystallites. This hypothesis was also supported by the IR spectra due to shifting of the water peaks. In our study such an effect is unclear from the positions of the stretching and bending modes of hydroxide species due to the low sensitivity of Raman to these bands. It is seen in this investigation that the (020) XRD peak of boehmite changes with ageing to a value that is closer to the values for gels that have been peptised. This observation is seen to support the observations of Zakharchenya.[18]

Table 2 Band component analysis of the low wavenumber region of the Raman spectra of the aged hydrolysates

	Band position/cm^{-1}				
	Ageing time/h				
Hydrolysate nature	0	0.5	1	2	4
Refluxed hydrolysates aged at 75 °C	352	354	355	355	356
	387	390	387	385	385
	414	414	410	408	406
	440	436	438	438	436
	466	470	471	472	474
	501	501	501	501	501
	547	531	582	534	526
Washed hydrolysates aged at 75 °C	333	333	333	333	333
	352	355	355	355	355
	405	414	413	403	405
	450	457	455	450	452
	470	479	475	468	474
	491	496	495	493	493
	544	503	505	528	515
	676	673	679	673	675
Refluxed hydrolysates aged at 85 °C	352	355	356	536	357
	389	388	385	389	390
	417	409	403	407	410
	440	438	439	435	436
	470	474	475	477	479
	502	501	501	501	502
	543	526	512	533	543
Washed hydrolyses aged at 85 °C	317	333	333	333	333
	349	354	355	355	356
	405	403	404	404	405
	456	450	450	456	451
	471	471	467	na	469
	493	492	493	492	493
	516	517	516	540	528

Doss and Zallen attribute the change in the FWHM of the 356 cm^{-1} peak to finite size effects due to crystal growth.[22] In this study, it is suggested that crystal growth does occur, but this crystal growth does not account for the increased peptisability of the hydrolysates. Finite crystal growth experiments show an increase in the size of the crystal domains. Although this is seen in these experiments the crystals of boehmite are highly distorted, thus lowering the crystal domain size. The crystal domain sizes do increase by a dissolution process but the main process involved in this study is likely to be a fracturing process. The ageing effect seen in the Raman spectra of the hydrolysates may be due to distortions in the crystalline lattice, which lower the crystal domain size. Pierre and Uhlmann suggest that the existence of a folded, distorted structure for amorphous aluminium (oxy)hydroxide.[11,12] This structure is proposed to straighten, and it is suggested in this study that the structure straightens *via* a fracturing and dissolution process of highly distorted crystals. The large distorted crystals contain large amounts of stacking defects along the 020 plane of boehmite. These defects represent regions of high strain, which must fracture to relieve stress. This causes the elimination of the defects in the lattice allowing better packing of layers. The increased peptisability of the hydrolysate can then be thought of as the strengthening of the hydrogen bonding along the 010 planes in the hydrolysates, which then allows for the redistribution of electron density in boehmite, indicative of the peptisation process. In this study it has been seen that these strained sites in the 020 plane of boehmite play such an important role in the peptisability of boehmite since an unstrained aged sample will even peptise at 35 °C. This is in stark contrast to the strained, un-aged system, which can only be peptised at high temperatures.[1]

It is seen from the plot of FWHM *versus* ageing time (Fig. 8) that the FWHMs of the refluxed hydrolysates are larger than those of the washed hydrolysates. This might suggest that the degree of crystallisation of the refluxed hydrolysates is less than that of the washed samples.A more likely explanation is, however, that the increased FWHM of the 355 cm^{-1} Raman band in the refluxed pseudoboehmite is most probably due to overlap of the broad 356 cm^{-1} Raman band for *sec*-butanol. The FWHM values of the 355 cm^{-1} band of the hydrolysates prepared at 85 °C show larger FWHM values than do the hydrolysates prepared at 75 °C. This is likely to be due to the fast precipitation of the pseudoboehmite causing extra distortions in the crystalline lattice. This is also seen in the peptisability of the alumina hydrolysates, with un-aged samples prepared at 75 °C peptising faster than samples prepared at 85 °C. The particle size of hydrolysates prepared at 85 °C is also likely to be larger causing the hydrolysate to be harder to peptise. It is also seen that the hydrolysates aged at 85 °C show larger particle sizes, as measured from dynamic light scattering (DLS) measurements, after 4 h of ageing due to their increased solubility at higher temperatures. Assih *et al.*[21] found the Raman spectra of pseudoboehmite sols to be similar to those of boehmite. They hypothesised that the hydrogen bonds in the pseudoboehmite lattice were made up of a wide distribution of hydrogen bond lengths as reflected by a large width of the hydroxy stretching frequencies at 3000–3800 cm^{-1}. This, however, is ignoring the possibility of irregular inter-layer water hydrogen bonding or the appearance of different co-ordination modes of water. Also expected would be an overlap of the ν_1, ν_3 and $2\nu_2$ bands as well as any overtones of the bending modes for the OH bending modes of the alumina.

The experiments conducted by Zakharchenya[18] found that peptisation caused an increase in the hydrogen bond strength in the pseudoboehmite, seen by a reduction in the inter-planar distances in the pseudoboehmite hydrolysates. It was hypothesized that peptisation results in the removal of inter-planar water, which would lead to the decrease in the crystal spacing as observed by XRD along the 010 plane of pseudoboehmite.

Zakharchenya postulated that surface charge formation caused a redistribution of electron density in boehmite, which results in an increase in the hydrogen bonding between crystallites. This hypothesis was also supported by the shifting positions of the water peaks seen in IR spectra. This redistribution of electron density described by Zakharchenya may play a part in the observations by Assih *et al.* This group did not find some of the vibrations described by Kiss *et al.* in the lattice vibrations of Al–O. It was probable the perturbation occurred due to the disruption of the crystalline lattice by water, as well as to some extent by poor crystallisation. Overlap with water libration and translational modes would also be expected. There is also another hindering effect when dealing with colloids derived from metal alkoxides in alcohols. The addition of metal alkoxides, in these cases usually aluminium *sec*-butoxide, to water results in a hydrolysis reaction which leads to the formation of the (oxy)hydroxide pseudoboehmite and alcohol. This organic alcohol has Raman-active bands in the region 1600–200 cm^{-1}, which are strong and may mask other bands of the spectrum. This alcohol may also bind to the alumina surface *via* hydrogen bonding. In such cases, it would be expected that the stretching modes should be shifted to higher frequencies and the bending modes to lower frequencies.

4 Conclusion

Alumina oxy(hydroxide) hydrolysates were formed from the hydrolysis of tri-*sec*-butoxyaluminium(III) dissolved in anhydrous dibutyl ether. These hydrolysates were aged for times up to 4 h. X-Ray diffraction showed that the alumina oxy(hydroxide) was boehmite. The variation of the peak width is related to the increase of crystallinity upon ageing. The *d*-spacings of the hydrolysates varied with the ageing time due to the incorporation of water into the inter-layer spaces. Thermal analysis patterns of the aged alumina (oxy)hydroxy hydrolysates were similar to that of boehmite. Raman spectroscopy also provided information about the increase in crystallinity with ageing time. Changes in the bandwidths of the boehmite peaks are attributed to finite size effects. The effects of ageing result in changes to the peptisability of the alumina hydrolysates.

The important research undertaken is based upon an *in-situ* study, in contrast to the studies of Kiss *et al.*[17] and Doss and Zallen.[22] In this research the Raman spectra were obtained *in-situ* without drying the samples before undertaking the analyses. Thus the spectra are obtained for the wet hydrolysates as they are aged without removing the samples from the Raman spectrometer.

Acknowledgements

The Centre for Instrumental and Developmental Chemistry, of the Queensland University of Technology is gratefully acknowledged for financial support for this project. The Australian Institute for Nuclear Science and Engineering (AINSE) is acknowledged for financial support of this project.

References

1 B. B. Yoldas, *J. Appl. Chem. Biotechnol.*, 1973, **23**, 803.
2 G. C. Bye and J. G. Robinson, *Kolloidn. Zh.*, 1964, **198**, 53.
3 W. A. Deer, R. A. Howie and J. Zussman, *An introduction to the rock forming minerals*, Addison Wesley Longman, Harlow, UK, 1996, pp. 571–572
4 E. Calvet, P. Boivinet, M. Noel, H. Thibon, A. Maillard and R. Tertain, *Bull. Soc. Chim. Fr.*, 1953, 99.
5 D. Papee, R. Tertain and R. Biais, *Bull. Soc. Chim. Fr.*, 1958, 1301.
6 M. Anast, A. Wong, J. M. Bell, B. Ben-Nissan, J. Cullen, L. Spiccia, D. De Villiers, I. Watkins, B. O. West and G. Johnson, Thin-Film Coatings *via* the Sol–Gel Process, *Key Eng. Mater.,*1990, **53–55**, 427
7 E. M. Rabinovich, *J. Mater. Sci.*, 1985, **20**, 4259.
8 J. Livage, M. Henry and C. Sanchez, *Sol–Gel Chemistry of the Transitional Metal Oxides*, Pergamon Press, Oxford, 1988, vol. 18, p. 259
9 R. L. Frost, J. T. Kloprogge and J. Szetu, *Thermochim. Acta*, 1999, **329**, 47.
10 R. L. Frost, J. T. Kloprogge, J. Szetu, H. Ruan and W. Martens, *Thermochim. Acta*, 2000, **362**, 37.
11 A. C. Pierre and D. R. Uhlmann, *J. Am. Ceram. Soc.*, 1987, **70**, 28.
12 A. C. Pierre and D. R. Uhlmann, *J. Non-Cryst. Solids*, 1986, **82**, 271.
13 W. Glaubitt, D. Sporn and R. Jahn, *J. Sol–Gel Sci. Technol.*, 1994, **2**, 525.
14 P. A. Buining, C. Pathmamanoharan, J. B. H. Jansen and H. N. W. Lekkerkerker, *J. Am. Ceram. Soc.*, 1992, **74**, 87.
15 P. P. Reichertz and W. J. Yost, *J. Phys. Chem.*, 1964, **14**, 495.
16 W. O. Milligan and J. L. McAttee, *J. Phys. Chem.*, 1956, **60**, 273.
17 A. B. Kiss, G. Keresztury and L. Farkas, *Spectrochim. Acta, Part A*, 1980, **36**, 653.
18 R. I. Zakharchenya, *J. Sol–Gel Sci. Technol.*, 1996, **6**, 179.
19 K. Wefers and G. M. Bell, *Oxides and hydroxides of aluminium, ALCOA Technical Paper No. 19*, Aluminium Company of America, Alcoa Centre, Pennsylvania, USA, 1972
20 S. Music, D. Dragcevic and S. Popovic, *Mater. Lett.*, 1996, **24**, 59.
21 T. Assih, A. Ayral, M. Abenoza and J. Phalippou, *J. Mater. Sci.*, 1998, **23**, 3326.
22 C. J. Doss and R. Zallen, *Phys. Rev. B*, 1993, **48**, 15 626.